CHEMISTRY

DOI: https://doi.org/10.36719/2707-1146/44/18-31

Tayyab Ashfaq Butt
College of Engineering, University of Hail
ta.butt@uoh.edu.sa

CANNABIS WEED BIOMASS ADSORBENT FOR BATCH ADSORPTION OF RO16 DYE FROM AQUEOUS SOLUTION

Abstract

This study examined Reactive Orange 16 (RO16) adsorption onto biochar made from cannabis weed biomass (CWB) in aqueous solutions. The adsorption process is negatively impacted by increasing temperatures, which results in a shift toward system stability and energy loss. This indicates that the process is exothermic, as demonstrated by negative enthalpy change (ΔH) values. The negative values of ΔG at different temperatures indicate spontaneous adsorption, highlighting the practicality of using CWB to remove RO16 in practical applications. Monolayer adsorption on homogeneous sites within the CWB structure is indicated by the Langmuir isotherm model, which accurately represents the adsorption behavior. CWB's effectiveness in RO16 adsorption was demonstrated by the greatest adsorption capacity of 33.45 mg/g. Additionally, the starting dye concentration, adsorbent dose, and solution pH have a major impact on the adsorption effectiveness of CWB. The significance of accessible adsorption sites is highlighted because optimal dye removal happens at lower dye concentrations and greater adsorbent dosages. Another important factor is pH; lower pH values result in increased removal efficiency because of the advantageous electrostatic interactions that occur between the protonated surface of CWB and the anionic dye. For removing RO16 dye from aqueous solutions, CWB shows a great deal of promise as an economical, effective, and long-lasting adsorbent.

Keywords: *Cannabis weed biochar, Reactive orange-16 dye, hemodynamic, kinetics of dye adsorption*

Introduction

The textile sector is ranked as a major contributor to environmentally harmful pollution, with 300, 000 t. of synthetic dyes entering into treatment plants whereby dyeing and finishing departments constitute about 20% of total industrial effluents (Rita Kant, 2012). It is reported by the Global Commission on the Economics of Water that the textile sector is contributing to the global scarcity of clean water globally around 40% by 2030 (Cairns, 2023). This not only pollutes the clean water but also induces photosynthetic impairment in aquatic plant (Saravanan et al., 2021). As the dyes are stable due to complex chemical structures, therefore, these are difficult to fade naturally (Carneiro, Nogueira, & Zanoni, 2007). Almost 10 to 15% of color entered into polluted water and besides health problems (Manzoor & Sharma, 2020), constituting a key environmental concern (Kyzas, Lazaridis, & Mitropoulos, 2012).

Numerous treatment methods have been tested on dyes treatment, for instance, fungal degradation (Sen, Raut, Bandyopadhyay, & Raut, 2016), ion exchange (Villalobos, Cid, & González, 2016), advanced oxidation processes (Navarro, Gabaldón, & Gómez-López, 2017) and adsorption (Gopinathan, Bhowal, & Garlapati, 2017; Qi, Yang, Xu, He, & Men, 2017). In these methods, the adsorption is the most prominent treatment method because of simple operation and facile application (Elsherbiny, 2013).

Several adsorbents have been used for dyes and organic pollutants adsorption from aqueous solutions such as sawdust (Khan, Sharma, Khan, & Mukhlif, 2014), corn cob (Salih, Abdul Kareem, & Anwer, 2022), waste woody biomass (Stjepanović et al., 2021), Pineapple plant stem (Chan, Tan, Abdullah, & Ong, 2016), herbaceous weeds (Khandare & Govindwar, 2015), low-cost filters

derived from invasive weed biomass of *Parthenium hysterophorus* (Kamath et al., 2022), and invasive plant biowaste (Nguyen et al., 2022). The invasive plant species cause huge economic losses to agriculture productivity, for instance, in India yearly monetary loss of US$ 16.8 billion to agriculture (Bang et al., 2022), therefore this pose a serious threat to the agricultural economy worldwide (Paini et al., 2016). This necessitates the transformation of invasive plant species to useful applications such as biosorbents for the removal of hazardous textile dyes from effluent streams. Cannabis weed is also recognized as an invasive agricultural weed (Canavan et al., 2022). This weed can be converted into low-cost adsorbent such as biochar. During this transformation, volatile matters get evaporated and porous carbon material is obtained. In this study, Cannabis weed biomass is converted into biochar without any chemical treatment. Finally, this was explored for the removal of reactive orange 16 dye from an aqueous solution in a batch reactor. The mechanism of dye adsorption was investigated using widely applied isotherms and kinetic models. The spontaneity of chemical reactions was investigated by thermodynamic studies.

Materials and Methodology

The investigation began with the collection of hemp biomass samples from nearby fields. These samples were then carefully cleaned, dried in the sun, and ground into a fine powder. Important characteristics like moisture content, volatile matter, ash content, and fixed carbon were then determined by a thorough proximate investigation. The next step involved the pyrolysis process, which produced biochar. Biochar was tested against reactive dyes as part of the adsorption investigation, and UV-visible spectrophotometry was used to measure the extent of dye removal. The effects of duration, dosage, pH, and initial dye concentration were all carefully investigated in order to determine how they affected the biochar's adsorption efficiency. Additionally, by closely examining various isotherms and reaction models, including the intra-particle diffusion model, pseudo-first order, pseudo-second order, Freundlich isotherm, and Langmuir isotherm, the underlying mechanism of the adsorption process was clarified.

Freundlich Isotherm:

qe=KfCe1/n

qe: Amount of dye adsorbed at equilibrium (mg/g).

Kf: Freundlich constant, representing adsorption capacity (mg/g) * (L/mg)^(1/n).

Ce: Equilibrium concentration of dye in solution (mg/L).

n: Freundlich exponent, indicating adsorption intensity.

Langmuir Isotherm:

qe=1+KLCeQmaxKLCe

qe: Amount of dye adsorbed at equilibrium (mg/g).

Qmax: Maximum monolayer adsorption capacity (mg/g).

KL: Langmuir constant, related to the energy of adsorption (L/mg).

Ce: Equilibrium concentration of dye in solution (mg/L).

Pseudo-first order:

log(qe−qt)=logqe−2.303k1t

qt: Amount of dye adsorbed at time t (mg/g).

1k1: Pseudo-first order rate constant (1/min).

t: Time (min).

Pseudo-second order:

qtt=k2qe21+qe1t

qt: Amount of dye adsorbed at time t (mg/g).

2k2: Pseudo-second order rate constant (g/mg·min).

t: Time (min).

Intra-particle Diffusion Model:

qt=kpt0.5+C

qt: Amount of dye adsorbed at time t (mg/g).

kp: Rate constant of intra-particle diffusion (mg/g·min^0.5).

t: Time (min).

C: Intercept representing boundary layer effect.

Results and Discussion

Experimental results from 30°C to 50°C show that Cannabis weed biomass (CWB) adsorbs Reactive Orange 16 (RO16) dye molecules. The adsorption effectiveness of CWB for RO16 was found to be 29.43% at a temperature of 30°C. Experiments conducted later at 50°C showed a decrease in adsorption efficiency, which reached 9.50%. The decrease in adsorption efficiency with increasing temperature, suggests that higher temperatures do not promote weaker interaction between the dye molecules and the adsorbent surface, resulting in lower adsorption efficiency (Hajira Haroon et al, 2020). Moreover, thermodynamic investigations are vital for comprehending the characteristics of the adsorption process. Using Equation 1, the equilibrium constant (Kc) was calculated. This Kc was then multiplied by the solution (water) density (ρw = 1000 g/L) to make it dimensionless (Rehman et al., 2018). Thermodynamic parameters utilizing Eqs. (2) and (3) can be used to compute changes in entropy (ΔS, kJ/mol), enthalpy (ΔH, kJ/mol), and Gibbs free energy (ΔG, kJ/mol).

$$l_n\, K_d(\rho_w) = \frac{q_e}{C_e} \quad (1)$$

$$\ln K_d(\rho_w) = \frac{\Delta S}{R} - \frac{\Delta H}{RT} \quad (2)$$

$$\Delta G = \Delta H - T\Delta S \quad (3)$$

The plot (ln Kd (ρw) vs 1/T) can be used to compute the parametric values of ΔH and ΔS. The adsorption process's endothermic or exothermic character is defined by ΔH, whereas the value of ΔG aids in determining whether the reaction is spontaneous or not. The unpredictability or disorder in the aqueous system at the solid-liquid interface during the adsorption process is reflected by ΔS. These characteristics are useful for assessing the appropriateness and practicality of a dye adsorption system. The adsorption dataset of each adsorbent against the target dye under a variable temperature range (30 to 50 °C), the initial dye concentration (30 mg/L), the adsorbent dosage (1 g/L), the equilibrium contacts time (variable for different adsorbents), the agitation speed (150 rpm), and the pH of the solution were used to calculate these parameters.

Table 1 Thermodynamic parameters for RO16 adsorption by cannabis weed biomass

ΔH (kJ mol^{-1})	ΔS (J mol^{-1} K^{-1})	ΔG (kJ mol^{-1})		
		T (K)		
		303.15	313.15	323.15
-36.55	70	-58.39	-59.11	-59.83

ISSN: 2707-1146
e-ISSN: 2709-4189

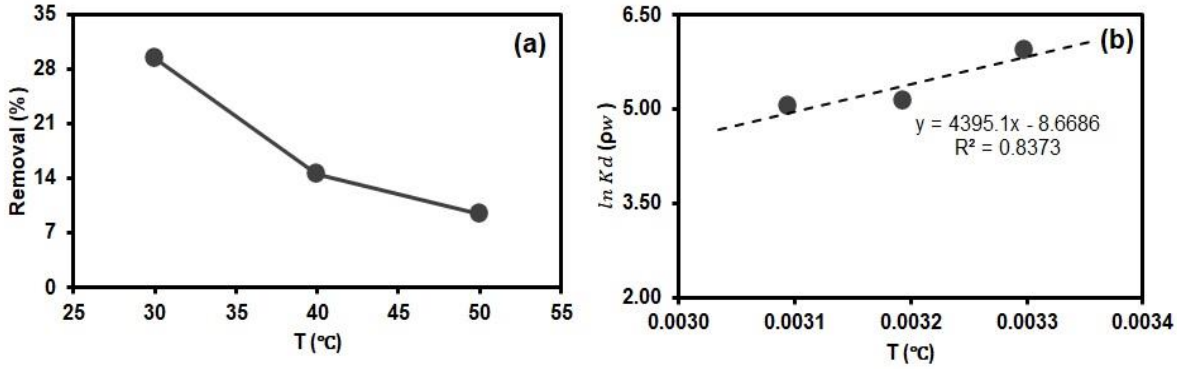

Figure 1. (a) Effect of Temperature on the adsorption of RO16 dye on CWB. (b) Thermodynamic plot for RO16 adsorption by cannabis weed biomass

The Figure 1 illustrates the thermodynamic plot, while the Table 1 provides a summary of the thermodynamic parameters for the adsorption of RO16 dye on cannabis weed biochar (CWB). The negative values of ΔH and positive values of ΔS° were observed when the temperature increased from 303.15 K to 323.15 K indicate that the adsorption process is exothermic and that there is an increase in randomness at the solid-liquid interface. This phenomenon can be attributed to the elevating temperature, which enhances the mobility of adsorbed ions or molecules within the solution. A high negative ΔG value indicates that adsorption process is exergonic and spontaneous in character, CWB loss energy and shift to lower and stable energy state.

Dyes Screening

Five distinct dye types were batch screened in order to choose dyes that would react with the biomass of CWB. Figure 2 illustrates how, in comparison to other dyes like RY145, RB2, MB, and Orange II, the RO16 has a significantly ($p = 0.01$) greater adsorbed content on the biomass at the highest rate of 44.5% in 120 minutes. As a result of these findings, RO16 dye was shown to be adsorbed most on the adsorbent and was chosen for additional research to test the performance of CWB under optimizing ambient conditions. Previously RO16 dye was adsorbed on the softwood bark in the aqueous solution (Averheim et al., 2024).

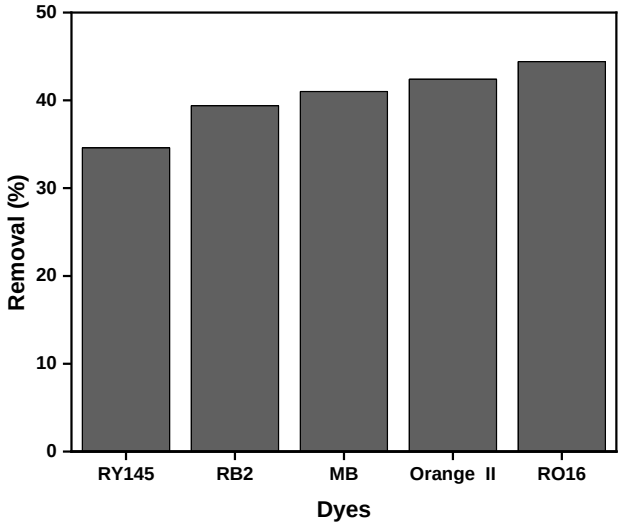

Figure 2. Screening of cannabis weed biomass against various textile dyes

Effect of time

As illustrated in Figure 3, the impact of contact time on the RO16 adsorption on CWB has been assessed. It only takes 120 minutes of contact time to reach equilibrium adsorption, or q_e = 44.5%.

Extending the contact period up to 240 minutes had no significant effect on the adsorption (p = 0.01). Hence, the duration of the remaining batch experiments was optimized to 120 minutes in order to achieve equilibrium. Since there are a lot of active sites on the adsorbent surface in the first 50 minutes of batch adsorption, the adsorption rate is high at the beginning and slows down as time goes on. Then, as the adsorbent's surface dye molecules reject the aqueous solution's dye molecules, the remaining empty sites get more difficult to be occupied, and the dye adsorption onto the CWB adsorbent decreases. In a previous study, tuja cone biomass exhibited a rapid adsorption behavior for methylene blue dye within the initial 50 minutes. Furthermore, this adsorption was optimized after 120 minutes of equilibrium time (Rehman et al., 2018).

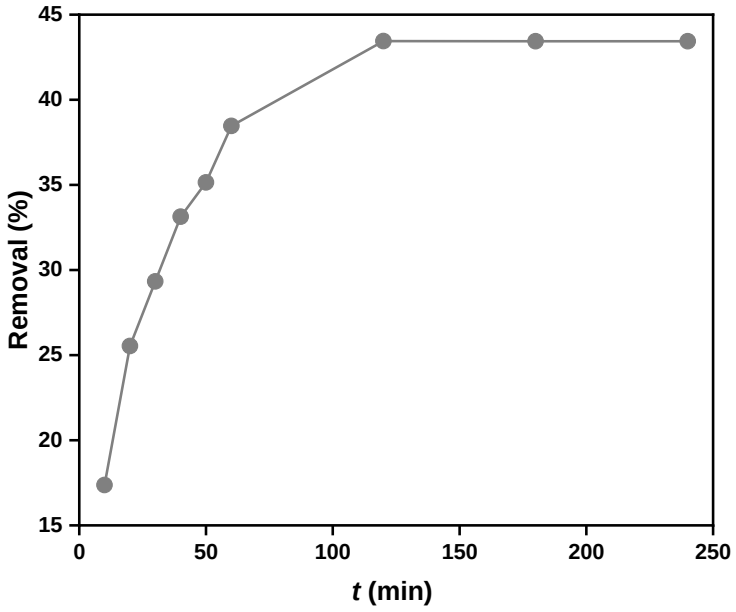

Figure 3 Effect of contact time on RO16 dye removal by Cannabis weed biomass

Effect of CWB dose

The overall efficacy of any adsorption process is significantly influenced by the amount of adsorbent utilized. As illustrated in the Figure 4, the amount of CWB adsorbent utilized influences the RO16 dye absorption from aqueous solution. A considerable increase in RO16 removal occurred from 34.82% to 61.91% when the quantity of adsorbent was increased from 0.4 to 3.2 g/L. The proliferation of binding sites associated with the quantity of the adsorbents present on the surface of CWB is the cause of this trend. As a consequence, a greater number of dye molecules are adsorbed onto the exposed adsorbent during the contact time. Previous research has shown similar patterns for RO16 dye utilizing *Ulva prolifera* (Ravindiran, Gaddam, & Sunil, 2022). The drop in binding ability is likely due to dye molecules building up on the CWB surface and the path distance for effective diffusion getting longer (Shah et al., 2020).

ISSN: 2707-1146
e-ISSN: 2709-4189

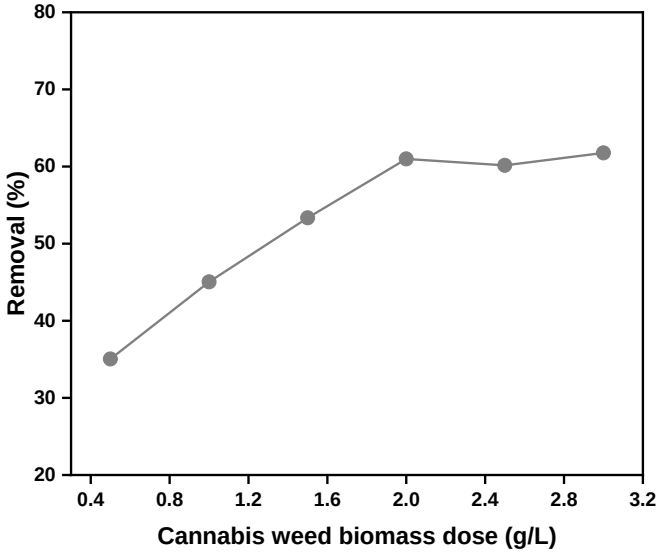

Figure 4. Effect of cannabis weed biomass dose on RO16 removal.

Effect of Initial Dye Concentration

As shown in Figure 5, the efficiency of CWB to eliminate RO16 at various initial concentration levels (25 to 150 mg/L) was investigated. It was discovered that increasing the dye concentration from 25 to 150 mg/L decreased the percentage of RO16 removed by CWB from 60% to 20.1% respectively. The increased availability of vacant binding sites on the surface of CWB led to a higher dye uptake per unit mass of adsorbent. The declining dye concentration can be attributed to the increased competition and conglomeration at the adsorbent surface, which provides resistance to mass transfer, caused by a greater number of dye molecules in aqueous phase.

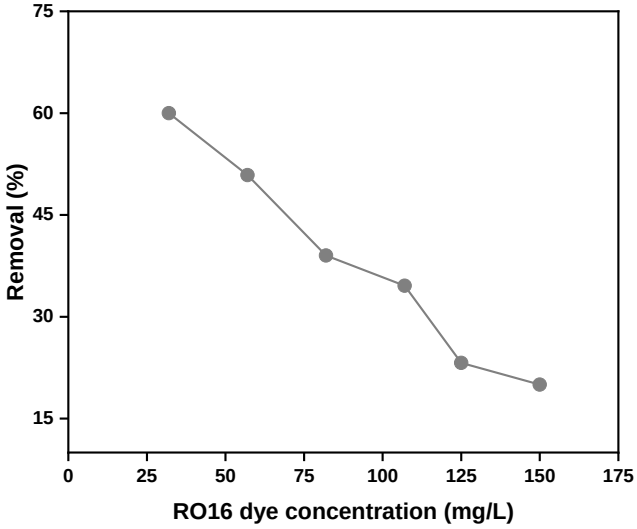

Figure 5. Effect of concentration on RO16 dye removal by cannabis weed biochar dose.

Effect of pH

In order to achieve efficient adsorption, RO16, an anionic dye, exhibits a pronounced attraction towards surfaces that are positively charged (Li et al., 2023). As shown in Figure 6, the dye adsorption peaked at 60.44% at pH 2 and dropped to 35.02% at pH 12, which is quite alkaline. The decline in concentration can be ascribed to the repulsive electrostatic interaction that likely occurs

between hydroxyl ions and anionic dye groups, which are probably in liquid phase. Carboxylic adsorption may also occur due to the protonated functional groups present on the surface of CWB at higher pH (Averheim et al., 2024).

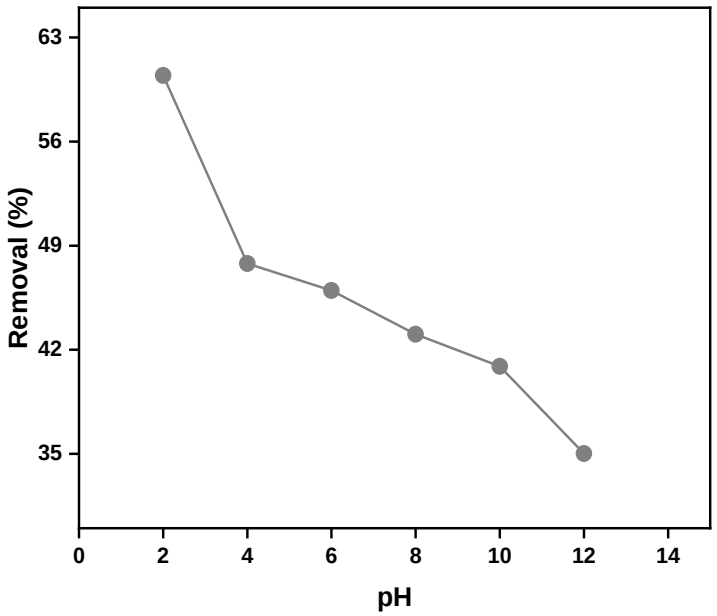

Figure 6. Effect of solution pH on RO16 removal by cannabis weed biochar

Adsorption Modelling

Mechanism and rate of adsorption was investigated by using different isotherm model and kinetic models.

Isotherm models

Based on the R^2 values presented in Table 2 and illustrated in Figure 7a, the Langmuir isotherm was identified as the most appropriate. Adsorbate monolayer formation, a layer of adsorbate with a single molecule thickness, over a predetermined number of adsorption sites is theoretically explained by the Langmuir isotherm. At equilibrium, the maximal adsorption capacity of 33.45 mg/g is achieved without any mutual contact between the adsorbate molecules. Once the adsorbate molecule fills an empty site, it is prevented from further attachment due to the establishment of a chemical bond (Langmuir 1918).

Since the adsorption process occurs in a uniform and singular layer, it significantly enhances the effectiveness of dye removal due to its higher adsorption efficiency (Mubashar Hussain Gardazi, Ali, Rehman, Ashfaq, & Bilal, 2017).

Furthermore, the free energy available for CWB (0.61) is linked to the constant Ka in the adsorption mechanism. Based on the value of dimensionless constant (where the separation factor = 0.07), the RO16 dye adsorption onto CWB is likely a favorable adsorption process (Rehman et al., 2018).

Table 2 Adsorption parameters for the removal of RO16 dye by cannabis weed biomass

Isotherms	Parameters	Values
Langmuir	q_{exp}	30.00
	q_{max}	33.45
	R_L	0.07
	K_a	0.08
	R^2	0.9957
Temkin	AT	1.37
	B=RT/bT	7.50
	*ln*AT	0.32
	R^2	0.9546
D-R	q_{DR} (mol/g)	28.14
	β $(mol/J)^2$	9×10^{-6}
	E (kJ/mol)	333.33
	R^2	0.9347
Freundlich	K_f	6.89
	N	2.97
	R^2	0.9046

Temkin isotherm indicates that lateral interaction between adsorbate molecules influences the adsorption process. The interaction lowers the heat of adsorption in the adsorbent's surrounding layers of adsorbate molecules.

The model is characterized by a uniform distribution of peak binding energies. A linear drop in the heat of adsorption will occur in the molecular layer of adsorbates around the adsorbent if low and high concentration thresholds are disregarded. For the RO16 dye adsorption onto CWB, the Figure 7b and Table 2 illustrate the graph curve and values of Temkin model constants derived from a linear fit.

The sorption heat in the adsorption system is reflected in the rate constant Bt; which is determined to be 1.36 kJ/mol, indicating that the lower RO16 facilitated an equitable distribution of lower bonding energies. As a result, the CWB surface sites experienced an increase in RO16 absorption on the CWB.

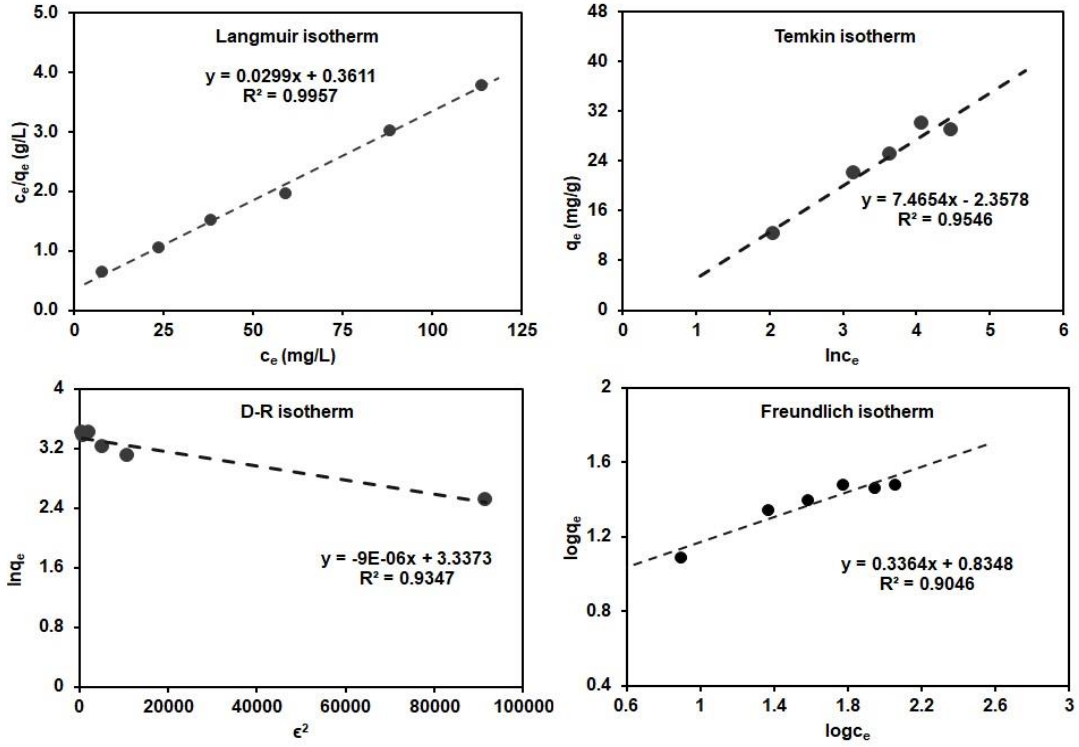

Figure 7 Isotherm models from experimental adsorption capacities of CWB for RO16 dye at variable initial concentrations

Moreover, a lower R^2 value for the q_{exp} compared to Langmuir isotherms in the adsorption system suggests that the model does not accurately represent the experimental data (Foo & Hameed, 2010). Table 2 and Figure 7 presents the D-R isotherm model fitness for RO16 on CWB. Chemisorption's primary driving force has been linked to a high value of E (>8 kJ/mol). The Langmuir chemisorption, in which chemical bonding dominated the potential adsorption mechanism, is consistent with this phenomena (Rehman et al., 2018).

The Freundlich isotherm postulates that contaminants will adsorb on the adsorbent's heterogeneous surface. The adsorption process's feasibility and intensity are determined by the parameters KF and n, which stand for relative adsorption capacity (6.89 dm^3/g) and heterogeneity factor (2.97) in Table 2. These constants were determined by looking at the plot of qe against Ce. In comparison to other models, the Freundlich model (Fig. 7d) showed a poor fit (R^2 = 0.904) to the equilibrium data. As a result, the adsorption demonstrated the CWB's monolayer coverage and uniform distribution of active sites (Mubashar Hussain Gardazi et al., 2017).

Kinetic models

Table 3 offers a summary of the parameters for several kinetic models, including the Elovich, intra-particle diffusion, and pseudo-second-order models. According to the pseudo-second order model, chemisorption involving valence forces through electron sharing or exchange between sorbent and adsorbate which could be the rate-limiting step. As summarized in Table 3 K_2 (g/mg/min) represents the pseudo-second order rate constant. The initial adsorption rate (h) and rate constant (K_2) were calculated by analyzing the intercept and slope of the plot t/qt vs. t. When compared to the intra-particle diffusion and elovich kinetic model, the R^2 values (0.879) showed that the adsorption of RO16 onto CWB less followed the pseudo-second order model, suggesting that this model was a poor fit for the experimental data (Bilal et al., 2013; Rehman et al., 2023).

The R^2 values demonstrate that the Elovich model provides a more accurate fit to the experimental data compared to the pseudo-second-order model. Greater R^2 values (0.887) indicate stronger concordance between the model and empirical observations. The alpha values imply a

ISSN: 2707-1146
e-ISSN: 2709-4189

higher number of active sites that are easily accessible on the CWB surface, as well as favorable conditions for adsorption. At increasing concentrations of adsorbate, the increased alpha value inhibits diffusion processes at higher concentrations of RO16.

Table 3 Kinetic parameter for RO16 adsorption onto CWB

Kinetic models	Equations	Parameters	Values
PSO	$\frac{t}{q_t} = \frac{1}{k_2 q^2{}_e} + \frac{t}{q_t}$	$q_{e\ cal}$	34.36
		K_2	0.0012
		h2	1.47
		R^2	0.9511
IPD	$q_t = k_p t^{1/2} + C$	C_i	2.27
		K_{diff}	2.21
		R^2	0.9859
Elovich	$q_t = \frac{1}{\beta}\ln(\alpha\beta) + \frac{1}{\beta} lnt$	A	0.06
		B	0.21
		R^2	0.8875

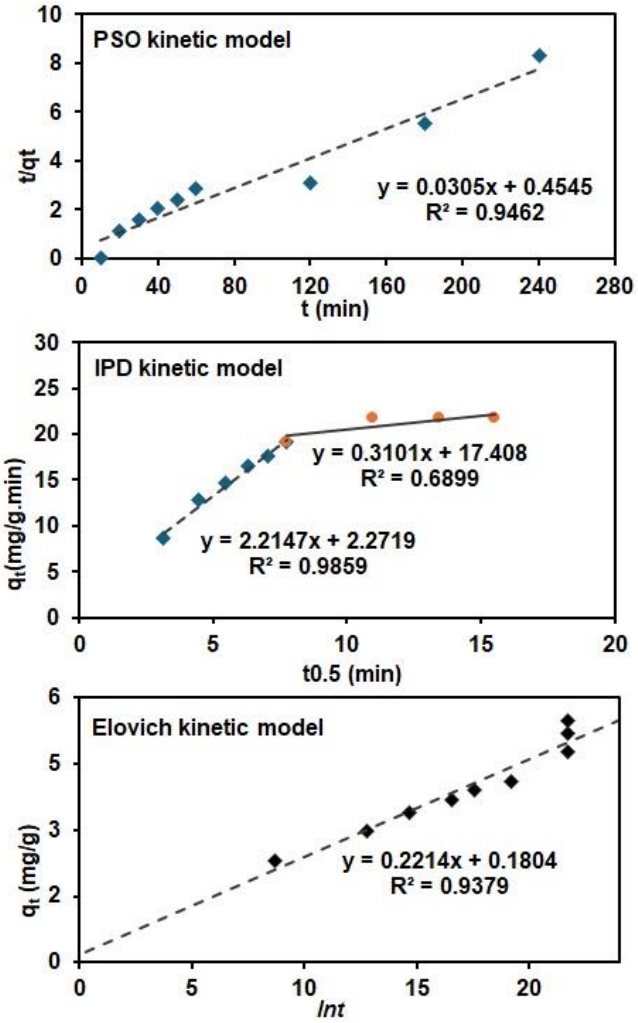

Figure 8. PSO, IPD and Elovich kinetic plot of RO16 removal by Cannabis weed biochar

The adsorption of aqueous pollutants in porous adsorbents is significantly influenced by intraparticle diffusion. To optimize the process parameters and understand the mass-transfer mechanisms, it is crucial to identify the rate-controlling step using intraparticle diffusion models. The linearization of the curve qt= ($t^{0.5}$) yields the initial intra-particle diffusion rate. The relationship between the plot of qt against $t^{0.5}$ may exhibit multi-linearity, as shown by (Hu, Ma, He, Liu, & Pei, 2024). This suggests that there are multiple steps involved in the adsorption processes. The initial phase is characterized by external surface adsorption, often known as the immediate adsorption stage. The second phase involves the progressive adsorption stage, when the diffusion within the particle is regulated by the rate. The third phase represents the ultimate state of balance, where the diffusion within the particles begins to decrease as a result of the exceedingly low concentration of solute in the solution (Dharmarathna & Priyantha, 2024). The validity of the intra-particle diffusion models was assessed using linear equation analysis Table 3) of log (q_e-q_t) versus t, (t/q_t) vs t, and q_t vs $t^{1/2}$. The connection that best describes the kinetic data is the one that elucidates the mechanism of dye adsorption in the solid phase (Zhu et al., 2023).

SEM and EDX Analysis

Figure 9 displays scanning electron microscope (SEM) images of the CWB surface at high magnification, both before (a) and after (b,c) the adsorption of RO16. The effective adsorption of RO16 is probably seen due to the even distribution of pores in CWB, which facilitates the process of dye adsorption. Following adsorption, the RO16 dye in the aqueous solution most likely filled the visible pores. The elemental composition of the CWB was primarily made up of C (63.68%), O (31.88%), Ca (2.40%) and K (0.93%) by weight prior to RO16 absorption. The confirmation of RO16's presence on CWB was established through changes in elemental composition following adsorption of RO16. The sample consisted of C (67.48%), O (27.38%), Ca (3.28%) and K (0.32%).

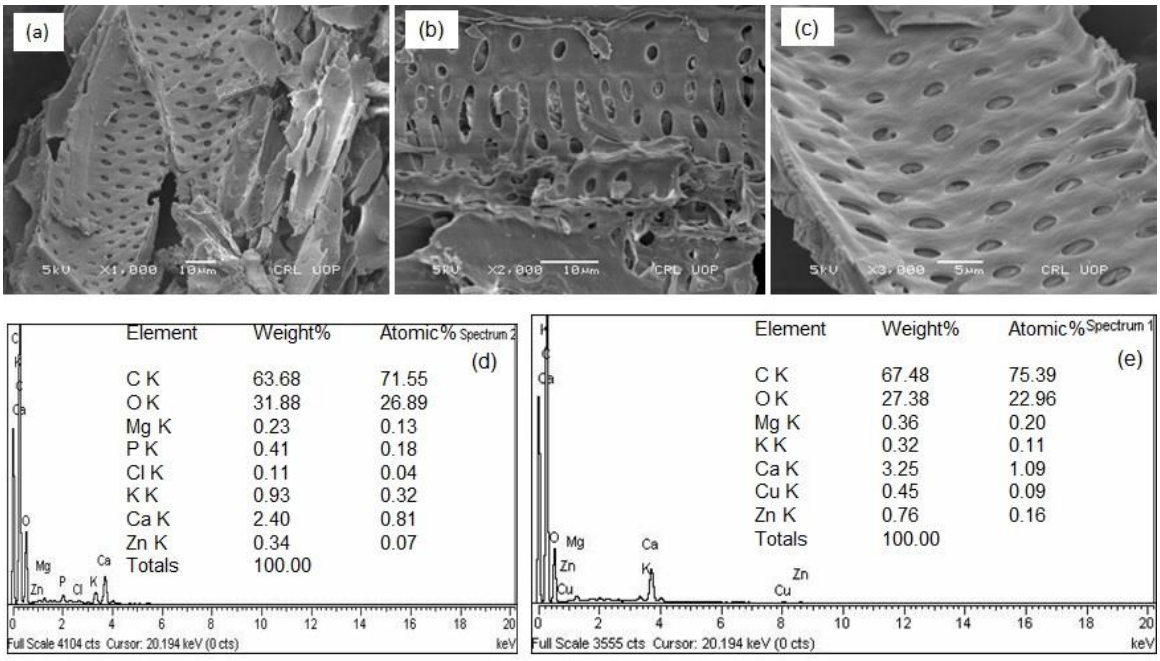

Figure 9. SEM micrographs of CWB before (a) and after (b,c) RO16 adsorption with corresponding EDX spectra (d) CWB before, (e) CWB after RO16 adsorption.

Conclusion

We illustrated RO16 adsorption onto the biochar of CWB in the aqueous solution. The adsorption process was found exothermic, as indicated by the negative values of ΔH. This suggests that higher temperatures do not favor the adsorption process, rather CWB adsorbent loose energy and system shift towards stability. The negative ΔG values across temperatures indicate that the adsorption process is spontaneous, which underlines the feasibility of using CWB for RO16

removal in practical applications. Furthermore, the Langmuir isotherm model fits the adsorption data well, indicating monolayer adsorption of RO16 on homogeneous sites within the CWB. The maximum adsorption capacity was found to be 33.45 mg/g, highlighting the effectiveness of CWB in adsorbing RO16. We also found that the adsorption efficiency of CWB is largely influenced by initial dye concentration, adsorbent dosage, and solution pH. Maximum dye removal was achieved at lower dye concentrations and higher adsorbent dosages, indicating that the availability of adsorption sites plays a crucial role. The adsorption is also highly pH-dependent, with higher removal efficiency at lower pH values due to favorable electrostatic interactions between the anionic dye and the protonated surface of CWB. In conclusion, CWB exhibits considerable potential as a low-cost, efficient, and sustainable adsorbent for the removal of RO16 dye from aqueous solutions.

References

1. Averheim, A., Dos Reis, G. S., Grimm, A., Bergna, D., Heponiemi, A., Lassi, U., & Thyrel, M. (2024). Enhanced biobased carbon materials made from softwood bark via a steam explosion preprocessing step for reactive orange 16 dye adsorption. Bioresource Technology, 130698.
2. Bang, A., Cuthbert, R. N., Haubrock, P. J., Fernandez, R. D., Moodley, D., Diagne, C., Courchamp, F. (2022). Massive economic costs of biological invasions despite widespread knowledge gaps: a dual setback for India. Biological Invasions, 24(7), 2017-2039. doi:10.1007/s10530-022-02780-z
3. Bilal, M., Shah, J. A., Ashfaq, T., Gardazi, S. M. H., Tahir, A. A., Pervez, A., Mahmood, Q. (2013). Waste biomass adsorbents for copper removal from industrial wastewater—a review. Journal of Hazardous Materials, 263, 322-333.
4. Cairns, R. (2023). One-fifth of water pollution comes from textile dyes. But a shellfish-inspired solution could clean it up. Retrieved from CNN:
5. Canavan, S., Brym, Z., Brundu, G., Dehnen-Schmutz, K., Lieurance, D., Petri, T., Flory, S. (2022). Cannabis de-domestication and invasion risk. Biological Conservation, 274, 109709.
6. Carneiro, P. A., Nogueira, R. F. P., & Zanoni, M. V. B. (2007). Homogeneous photodegradation of C.I. Reactive Blue 4 using a photo-Fenton process under artificial and solar irradiation. Dyes and Pigments, 74(1), 127-132. doi:https://doi.org/10.1016/j.dyepig.2006.01.022
7. Chan, S.-L., Tan, Y. P., Abdullah, A. H., & Ong, S.-T. (2016). Equilibrium, kinetic and thermodynamic studies of a new potential biosorbent for the removal of Basic Blue 3 and Congo Red dyes: Pineapple (Ananas comosus) plant stem. Journal of the Taiwan Institute of Chemical Engineers, 61, 306-315. doi:https://doi.org/10.1016/j.jtice.2016.01.010
8. Dharmarathna, S., & Priyantha, N. (2024). Investigation of Boundary Layer Effect of Intra-Particle Diffusion on Methylene Blue Adsorption on Activated Carbon. Energy Nexus, 100294.
9. Elsherbiny, A. S. (2013). Adsorption kinetics and mechanism of acid dye onto montmorillonite from aqueous solutions: Stopped-flow measurements. Applied Clay Science, 83, 56-62.
10. Foo, K. Y., & Hameed, B. H. (2010). Insights into the modeling of adsorption isotherm systems. Chemical engineering journal, 156(1), 2-10.
11. Gopinathan, R., Bhowal, A., & Garlapati, C. (2017). Thermodynamic study of some basic dyes adsorption from aqueous solutions on activated carbon and new correlations. The Journal of Chemical Thermodynamics.
12. Hu, Q., Ma, S., He, Z., Liu, H., & Pei, X. (2024). A revisit on intraparticle diffusion models with analytical solutions: Underlying assumption, application scope and solving method. Journal of Water Process Engineering, 60, 105241.
13. Kamath, S. V., Manohara, H. M., Aruchamy, K., Maraddi, A. S., D'Souza, G. B., Santhosh, K. N., Nataraj, S. (2022). Sorption based easy-to-use low-cost filters derived from invasive weed biomass for dye contaminated water cleanup. RSC advances, 12(15), 9101-9111.

14. Khan, T. A., Sharma, S., Khan, E. A., & Mukhlif, A. A. (2014). Removal of congo red and basic violet 1 by chir pine (Pinus roxburghii) sawdust, a saw mill waste: batch and column studies. Toxicological & Environmental Chemistry, 96(4), 555-568.
15. Khandare, R. V., & Govindwar, S. P. (2015). Phytoremediation of textile dyes and effluents: current scenario and future prospects. Biotechnology Advances, 33(8), 1697-1714.
16. Kyzas, G. Z., Lazaridis, N. K., & Mitropoulos, A. C. (2012). Removal of dyes from aqueous solutions with untreated coffee residues as potential low-cost adsorbents: Equilibrium, reuse and thermodynamic approach. Chemical engineering journal, 189, 148-159.
17. Li, R., Chen, J., Zhang, H., Rehman, F., Siddique, J., Shahab, A., . . . Luo, L. (2023). Facile synthesis of magnetic-activated nanocomposites for effective removal of cationic and anionic dyes in an aqueous environment: An equilibrium isotherm, kinetics and thermodynamic studies. Chemical Engineering Research and Design, 189, 319-332.
18. Manzoor, J., & Sharma, M. (2020). Impact of textile dyes on human health and environment. In Impact of textile dyes on public health and the environment (pp. 162-169): IGI Global.
19. Mubashar Hussain Gardazi, S., Ali, M., Rehman, S., Ashfaq, T., & Bilal, M. (2017). Process optimization of hazardous malachite green (MG) adsorption onto white cedar waste: isotherms, kinetics and thermodynamic studies. Current Analytical Chemistry, 13(4), 305-316.
20. Navarro, P., Gabaldón, J. A., & Gómez-López, V. M. (2017). Degradation of an azo dye by a fast and innovative pulsed light/H 2 O 2 advanced oxidation process. Dyes and Pigments, 136, 887-892.
21. Nguyen, D. T. C., Tran, T. V., Kumar, P. S., Din, A. T. M., Jalil, A. A., & Vo, D.-V. N. (2022). Invasive plants as biosorbents for environmental remediation: a review. Environmental Chemistry Letters, 20(2), 1421-1451. doi:10.1007/s10311-021-01377-7
22. Paini, D. R., Sheppard, A. W., Cook, D. C., De Barro, P. J., Worner, S. P., & Thomas, M. B. (2016). Global threat to agriculture from invasive species. Proceedings of the National Academy of Sciences, 113(27), 7575-7579.
23. Qi, Y., Yang, M., Xu, W., He, S., & Men, Y. (2017). Natural polysaccharides-modified graphene oxide for adsorption of organic dyes from aqueous solutions. Journal of Colloid and Interface Science, 486, 84-96.
24. Ravindiran, G., Gaddam, K., & Sunil, K. (2022). Experimental investigation on reactive orange 16 removal using waste biomass of Ulva prolifera. Advances in Materials Science and Engineering, 2022, 1-8.
25. Rehman, S., Adil, A., Shaikh, A. J., Shah, J. A., Arshad, M., Ali, M. A., & Bilal, M. (2018). Role of sorption energy and chemisorption in batch methylene blue and Cu 2+ adsorption by novel thuja cone carbon in binary component system: Linear and nonlinear modeling. Environmental Science and Pollution Research, 25, 31579-31592.
26. Rehman, S., Yousaf, S., Ye, Q., Chenhui, L., Bilal, M., Shaikh, A. J., . . . Wu, P. (2023). Bentonite binding with mercury (II) ion through promotion of reactive oxygen species derived from manure-based dissolved organic matter. Environmental Science and Pollution Research, 30(10), 26107-26119.
27. Rita Kant, R. K. (2012). Textile dyeing industry an environmental hazard.
28. Salih, S. J., Abdul Kareem, A. S., & Anwer, S. S. (2022). Adsorption of anionic dyes from textile wastewater utilizing raw corncob. Heliyon, 8(8), e10092. doi:https://doi.org/10.1016/j.heliyon.2022.e10092
29. Saravanan, A., Kumar, P. S., Vo, D.-V. N., Jeevanantham, S., Karishma, S., & Yaashikaa, P. (2021). A review on catalytic-enzyme degradation of toxic environmental pollutants: Microbial enzymes. Journal of Hazardous Materials, 419, 126451.
30. Sen, S. K., Raut, S., Bandyopadhyay, P., & Raut, S. (2016). Fungal decolouration and degradation of azo dyes: A review. Fungal Biology Reviews, 30(3), 112-133.
31. Shah, J. A., Butt, T. A., Mirza, C. R., Shaikh, A. J., Khan, M. S., Arshad, M., Yaqoob, K. (2020). Phosphoric acid activated carbon from Melia azedarach waste sawdust for adsorptive

removal of reactive orange 16: Equilibrium modelling and thermodynamic analysis. Molecules, 25(9), 2118.
32. Stjepanović, M., Velić, N., Galić, A., Kosović, I., Jakovljević, T., & Habuda-Stanić, M. (2021). From waste to biosorbent: Removal of congo red from water by waste wood biomass. Water, 13(3), 279.
33. Villalobos, M. C., Cid, A. P., & González, A. M. H. (2016). Removal of textile dyes and metallic ions using polyelectrolytes and macroelectrolytes containing sulfonic acid groups. Journal of environmental management, 177, 65-73.
34. Zhu, Y., Cui, Y., Peng, Y., Dai, R., Chen, H., & Wang, Y. (2023). Preparation of CTAB intercalated bentonite for ultrafast adsorption of anionic dyes and mechanism study. Colloids and Surfaces A: Physicochemical and Engineering Aspects, 658, 130705.

Received: 27.03. 2024 Accepted: 04.05.2024